

# 000 001 REVISUAL-R1: ADVANCING MULTIMODAL REASON- 002 ING FROM OPTIMIZED COLD START TO STAGED RE- 003 INFORCEMENT LEARNING 004 005

006 **Anonymous authors**  
007 Paper under double-blind review  
008  
009  
010  
011  
012

## ABSTRACT

013 Inspired by the remarkable reasoning capabilities of Deepseek-R1 in complex tex-  
014 tual tasks, many works attempt to incentivize similar capabilities in Multimodal  
015 Large Language Models (MLLMs). However, they still struggle to activate com-  
016 plex reasoning. In this paper, rather than examining multimodal RL in isolation,  
017 we delve into current training pipelines and identify three crucial phenomena: 1)  
018 Effective cold start initialization is critical for enhancing MLLM reasoning. In-  
019 triguely, we observe that initializing with carefully selected text data alone can  
020 lead to performance surpassing many recent multimodal reasoning models, even  
021 before multimodal RL. 2) Standard GRPO applied to multimodal RL suffers from  
022 gradient stagnation, which degrades both training stability and performance. 3)  
023 A final text-only RL tuning stage, conducted after the multimodal RL phase, is  
024 effective at further sharpening multimodal reasoning capabilities. Capitalizing on  
025 these insights, we introduce **ReVisual-R1**, achieving a new state-of-the-art among  
026 open-source 3B and 7B MLLMs on challenging benchmarks, including Math-  
027 Verse, MathVision, WeMath, LogicVista, DynaMath, and challenging AIME2024  
028 and AIME2025. This paradigm demonstrates robust scalability, proving effective  
029 at both 7B and 3B scales. Our findings chart a new course for training pow-  
030 erful multimodal reasoners, demonstrating that a carefully orchestrated, multi-  
031 stage strategy is key to unlocking their full potential. Our code is available at  
032 [https://anonymous.4open.science/r/Revisual\\_R1-7375](https://anonymous.4open.science/r/Revisual_R1-7375).  
033  
034

## 1 INTRODUCTION

035 Recently, the field of large language models (LLMs) has witnessed significant advancements in  
036 complex cognitive reasoning (Zeng et al.; Yan et al., 2025; Zhang et al., 2025a), notably exemplified  
037 by reasoning models like DeepSeek-R1 (Guo et al., 2025a). These models successfully leveraged  
038 Reinforcement Learning (RL) to facilitate the self-emergence of intricate reasoning abilities in text-  
039 only models. A natural and ambitious next step is to extend this RL paradigm to Multimodal Large  
040 Language Models (MLLMs), with the goal of unlocking a similar leap in multimodal cognitive  
041 abilities (Huang et al., 2025; Meng et al., 2025b; Xia et al.; Peng et al., 2025).

042 However, this ambition has been met with a formidable challenge. The direct application of text-  
043 centric RL techniques to MLLMs has yielded diminishing returns, suggesting that the path to mul-  
044 timodal reasoning is not a simple matter of architectural extension. A fundamental question arises:  
045 *how does one cultivate the abstract linguistic skill while simultaneously grounding it in the continu-  
046 ous, high-dimensional space of visual perception?* Naive co-training often results in a compromise,  
047 where neither modality's potential is fully realized. Motivated by this critical impasse, we undertake  
048 a rigorous dissection of the MLLM training pipeline. Our investigation uncovers three foundational  
049 insights that, when addressed in concert, chart a new and more effective course for developing pow-  
050 erful multimodal reasoners.

051 First, we observe that sufficient cold start initialization is indispensable for effectively cultivating the  
052 reasoning ability of MLLMs. Conventional cold-start phases for MLLMs often rely on simplistic  
053 visual and textual pre-training corpora (Yang et al., 2025; Huang et al., 2025; Wang et al., 2025;  
Deng et al., 2025; Chen et al., 2025b). This initial deficit critically hinders the subsequent RL

054 stages from eliciting sophisticated, self-critical reasoning patterns. To unlock deeper deliberative  
 055 reasoning in MLLMs, an enriched cold-start initialization is therefore not merely beneficial but  
 056 indispensable. Specifically, initializing with carefully selected text data that instills foundational  
 057 reflective capabilities and the capacity for extended Chain-of-Thought (CoT) reasoning proves to be  
 058 a powerful strategy. Intriguingly, such targeted textual initialization allows our model to surpass the  
 059 multimodal reasoning performance of many recent multimodal reasoning models.

060 Second, we identify that the standard Group Relative Policy Optimization (GRPO) algorithm (Shao  
 061 et al., 2024), commonly applied for multimodal RL, suffers from a gradient stagnation problem.  
 062 This issue significantly degrades both the training stability and the ultimate performance of the multi-  
 063 modal RL phase. To address this fundamental limitation and improve the efficacy of multimodal RL,  
 064 we propose Prioritized Advantage Distillation (PAD). PAD is designed to mitigate gradient stagna-  
 065 tion by strategically filtering out zero-advantage samples and re-weighting informative trajectories,  
 066 thereby focusing the learning process on more impactful data and improving training stability.

067 Third, we discover that conducting further post-training using text RL after the multimodal RL  
 068 training phase can further enhance multimodal reasoning ability. This stage acts as a polishing  
 069 step, sharpening the model’s linguistic expression and logical consistency without eroding the newly  
 070 acquired visual grounding. It consolidates the model’s capabilities, leading to a synergistic whole  
 071 greater than the sum of its parts.

072 Synthesizing these insights, we propose a principled, three-stage training curriculum that strategi-  
 073 cally sequences these learning phases: (1) a text-centric cold-start to forge a powerful reasoning  
 074 engine, (2) a multimodal RL phase with PAD to ground this engine in vision, and (3) a text-only RL  
 075 refinement to consolidate and polish the integrated skills. The culmination of this methodology is  
 076 **ReVisual-R1**, the first 7B-parameter open-source MLLM architected around this curriculum. Exten-  
 077 sive experiments on a suite of challenging benchmarks, including MathVerse (Zhang et al., 2024b),  
 078 MathVision (Wang et al., 2024a), MathVista (Lu et al., 2023a), DynaMath (Zou et al., 2025), We-  
 079 Math (Qiao et al., 2024a), and LogicVista (Xiao et al., 2024), as well as the AIME24/25 (Li et al.,  
 080 2024), GPQA (Rein et al., 2024), MATH-500 (Hendrycks et al., 2021) benchmark, confirm that  
 081 ReVisual-R1 significantly outperforms much larger public models. We further validate the scalabil-  
 082 ity of our framework by demonstrating its effectiveness at the 3B model scale.

083 To summarize, our contributions are as follows:

- 084 • We challenge the conventional MLLM training paradigm by demonstrating that a text-centric,  
 085 high-difficulty cold-start is the crucial, and previously overlooked, foundation for unlocking elite  
 086 multimodal reasoning.
- 087 • We identify the fundamental problem of gradient stagnation in multimodal RL and propose Pri-  
 088 oritized Advantage Distillation (PAD), a novel and effective solution that stabilizes training and  
 089 enhances sample efficiency.
- 090 • We present ReVisual-R1, an open-source 7B MLLM developed through a principled three-stage  
 091 curriculum. This approach uniquely cultivates deep, self-reflective reasoning and robust visual  
 092 grounding, enabling ReVisual-R1 to achieve state-of-the-art performance on complex multimodal  
 093 reasoning tasks, rivaling even larger or proprietary models.

## 094 2 PRELIMINARIES

097 In this section, we first formulate the task setting and key concepts in the multimodal reasoning  
 098 problem. Then, we describe the base training algorithm framework used in our method.

### 100 2.1 MULTIMODAL REASONING FORMULATION

102 In multimodal reasoning tasks, the input can be represented as  $x = (v, q)$ , where  $v$  denotes the visual  
 103 content, and  $q$  denotes the textual query. Our work aims to guide a MLLM to generate a multi-step,  
 104 self-reflective reasoning process  $t$ , which ultimately assists the model in producing a solution  $y$  that  
 105 correctly answers the query based on the multimodal input.

106 Formally, we aim to learn a policy  $\pi_\theta(y|x)$ , parameterized by  $\theta$ , which maps the input question  
 107 space  $\mathcal{X}$  to the solution space  $\mathcal{Y}$ . Our objective is to optimize the model parameters such that the  
 expected reward  $r(y, x)$  over the output distribution is maximized:

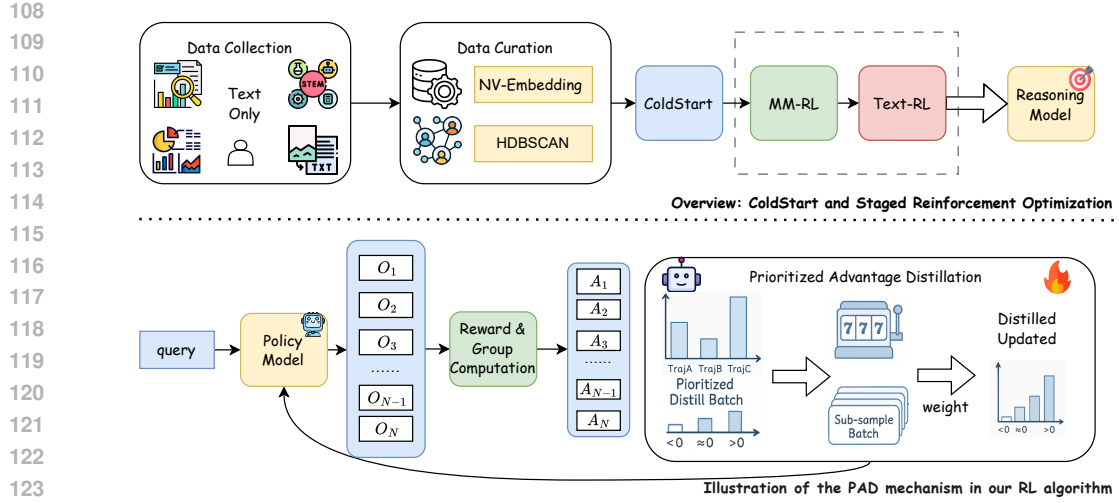


**Figure 1:** (Top): the overview of our proposed ReVisual-R1 framework. After collecting and curating data, ReVisual-R1 contains cold start and staged reinforcement learning. (Bottom): the process of our proposed prioritized advantage distillation (PAD) for multimodal reinforcement learning.

$$\theta^* = \arg \max_{\theta} \mathbb{E}_{x \sim \mathcal{D}} \mathbb{E}_{y \sim \pi_{\theta}(y|x)} [r(y, x)] \quad (1)$$

where  $\mathcal{D}$  represents the distribution of multimodal reasoning tasks. Similar to Deepseek R1 (Guo et al., 2025a), we mainly use rule-based reward,  $r(x, y) = 1$  if  $y$  is correct, otherwise  $r(x, y) = 0$ .

## 2.2 GROUP RELATIVE POLICY OPTIMIZATION

Group Relative Policy Optimization (GRPO) extends traditional policy optimization methods by organizing training samples into groups and optimizing policies relative to reference models within each group, offering several advantages for training language models on complex reasoning tasks.

Formally, given a batch of samples  $\mathcal{B}$ , GRPO divides them into  $K$  groups  $\{\mathcal{G}_1, \mathcal{G}_2, \dots, \mathcal{G}_K\}$  based on certain criteria. For each group  $\mathcal{G}_i$ , we maintain both a policy model  $\pi_{\theta}$  and a reference model  $\pi_{\theta_{\text{ref}}}$ . The GRPO objective for each group is formulated as:

$$\mathbb{E}_{x \sim \mathcal{G}_i} \mathbb{E}_{y \sim \pi_{\theta}(y|x)} \left[ \min \left( \frac{\pi_{\theta}(y|x)}{\pi_{\theta_{\text{ref}}}(y|x)} \hat{A}(x, y), \text{clip} \left( \frac{\pi_{\theta}(y|x)}{\pi_{\theta_{\text{ref}}}(y|x)}, 1 - \epsilon, 1 + \epsilon \right) \hat{A}(x, y) \right) \right] \quad (2)$$

where  $\epsilon$  is a hyperparameter controlling the size of the trust region, and  $\hat{A}(x, y)$  is the group-specific advantage function. For each input  $x$  with  $G$  generated responses  $\{y_1, \dots, y_G\}$  within a group, the advantage for response  $y_i$  is defined as:

$$\hat{A}(x, y_i) = \frac{r(x, y_i) - \text{mean}(\{r(x, y_1), \dots, r(x, y_G)\})}{\text{std}(\{r(x, y_1), \dots, r(x, y_G)\}) + \epsilon} \quad (3)$$

where  $\epsilon$  is a small constant for numerical stability. This relative advantage is then used within a clipped surrogate objective function.  $r(x, y_i)$  represents the reward for response  $y_i$  to input  $x$ . This advantage function measures how much better a specific response is compared to the average performance within its group, normalized by the group's reward variance.

## 3 OPTIMIZED COLD START FOR MULTIMODAL REASONING

In this section, we first show an intriguing finding in the cold start of multimodal reasoning in Section 3.1, paving the way for the strategy of our data curation pipeline in Section 3.2. As shown in Figure 1, our Revisual-R1 includes a cold start stage followed by staged reinforcement learning.

162  
163  
**Table 1:** Textual and multimodal reasoning datasets source of our GRAMMAR.  
164

Source	Multimodal Samples   Source	Samples	Source	Text-only Samples   Source	Samples
FigureQA (Kahou et al., 2018)	100K	Super-CLEVR (Li et al., 2023)	30K	Big-Math-RL (Albalak et al., 2025)	251K
MAVIS (Zhang et al., 2025b)	218K	TabMWP (Lu et al., 2023b)	38K	Big-Math-RL-U	35K
GeoQA (Chen et al., 2021)	5K	UniGeo (Chen et al., 2022)	16K	OpenThoughts (Team, 2025)	114K
Geometry3K (Lu et al., 2021a)	2.1K	MultiMath (Peng et al., 2024)	300K	DeepMath (He et al., 2025)	103K
IconQA (Lu et al., 2021b)	107K			OpenR1-220k (Face, 2025)	220K
				GAIR_LIMO (Ye et al., 2025)	0.8K
				s1K-1.1 (Muenninghoff et al., 2025)	1K
				OpenMathR (Moshkov et al., 2025)	3,200K
				OrcaMath (Mitra et al., 2024a)	200K
				NuminaMath-CoT (Li et al., 2024)	859K

168  
169  
170 

### 3.1 PRELIMINARY STUDY OF COLD START

171 To investigate the effectiveness of cold-start  
172 training (Guo et al., 2025a), we first collect  
173 two open-source cold-start multimodal datasets,  
174 Vision-R1 (Huang et al., 2025) and R1-One-  
175 Vision (Yang et al., 2025), along with two  
176 cold-start textual datasets, DeepMath (He et al.,  
177 2025) and OpenR1-Math (Face, 2025). Then  
178 we randomly sample 40,000 instances from  
179 these datasets to fine-tune Qwen2.5-VL-7B-  
180 Instruct (Bai et al., 2025). The fine-tuned mod-  
181 els are subsequently evaluated on multimodal  
182 reasoning benchmarks (MathVerse and MathVi-  
183 sion) as well as textual reasoning benchmarks  
184 (AIME24 and Math500). The experimental  
185 outcomes and average performance enhance-  
186 ments from the multimodal and textual cold-  
187 start datasets are illustrated in Figure 2.

188 The results in Figure 2 reveal that models  
189 trained with text-only cold start data exhibit  
190 substantial improvements in both textual and  
191 multimodal reasoning tasks. In contrast, mod-  
192 els trained solely on multimodal datasets, such as  
193 Vision-R1 and R1-One-Vision, show limited gains  
194 in both multimodal and textual reasoning. This suggests that the complexity and patterns presented  
195 by textual cold start data may better stimulate the models’ reasoning capabilities.

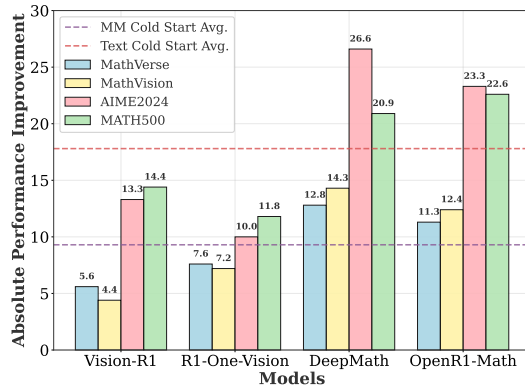
196 To further investigate this observation, we perform an analysis using a subset of 100 examples sam-  
197 pled from the Vision-R1 (Huang et al., 2025) and DeepMath (He et al., 2025) datasets. Specifically,  
198 we analyze the response lengths and pass rates of the doubaol-1.5-thinking-pro-vision model (Seed  
199 et al., 2025) on these samples. Responses to textual prompts from DeepMath averaged 8,207.76  
200 tokens, which is substantially longer than the 821.48 tokens generated in response to multimodal  
201 prompts from Vision-R1. Moreover, the pass rate for Vision-R1 is 96.00%, whereas DeepMath  
202 achieves a pass rate of only 75.0%. These findings further indicate that current multimodal cold  
203 start datasets may lack sufficient complexity to inspire advanced reasoning capabilities of reasoning  
204 models. Therefore, in this paper, we adopt textual-only data for the cold start stage.

205  
206 

### 3.2 GRAMMAR: GENERALIZED MULTIMODAL REASONING DATASET

207 Informed by Section 3.1, in this paper, we develop the Generalized Multimodal Reasoning Dataset  
208 (GRAMMAR) to enhance the generalization of reasoning capabilities in multimodal models. Specif-  
209 ically, the GRAMMAR dataset consists of two components. For the cold-start stage, it includes  
210 283K diverse and complex textual samples that feature explicit reasoning paths. For reinforcement  
211 learning with a verifiable reward, it contains an additional 31K complex textual examples and 21K  
212 multimodal questions, all of which are annotated with ground truths.

213 As shown in Figure 1, the construction of GRAMMAR involves a multi-stage curation pipeline.  
214 We begin by amassing open-source reasoning datasets in Table 1, spanning various difficulty levels.  
215 This initial collection underwent rule-based filtering to ensure answer verifiability, excluding items  
216 like proof problems and those with difficult-to-verify ground truths. Subsequently, Qwen2.5-VL-  
217 7B-Instruct is employed for initial pruning of overly simple or complex questions. Then, Qwen2.5-



218  
219 **Figure 2:** Absolute performance improvement on  
220 Qwen2.5-VL-7B-Instruct across textual and multi-  
221 modal reasoning tasks. The purple and red dashed lines  
222 represent the average absolute gains of VisionR1/R1-  
223 One-Vision and DeepMath/OpenR1-Math over the  
224 baseline, respectively, across four reasoning tasks.

VL-32B-Instruct is used to assess the remaining samples to classify them into ten difficulty levels. To maximize data diversity and minimize redundancy, we encoded questions using NV-Embedding-V2 (Lee et al., 2024), applied HDBSCAN (Campello et al., 2013) for clustering, assigned topics to clusters via Qwen2.5-7B-Instruct, and performed balanced sampling across both topics and difficulty strata.

## 4 STAGED REINFORCEMENT OPTIMIZATION (SRO)

In Section 3, our data investigations and the curation of the GRAMMAR dataset highlight the necessity of high-quality, reasoning-focused data for developing advanced MLLM capabilities. In this section, we introduce Staged Reinforcement Optimization (SRO) to systematically cultivate robust reasoning and diverse competencies in MLLMs. Specifically, SRO contains two stages including multimodal RL and subsequently textual RL.

### 4.1 STAGE 1: MULTIMODAL RL

After the cold start training, the SRO framework commences with a dedicated Multimodal Reinforcement Learning (MRL) phase. This initial stage is pivotal for enabling the MLLM to ground textual concepts in visual information and execute cross-modal reasoning, primarily using the multimodal samples from our GRAMMAR dataset. We employ GRPO as the core RL algorithm for this phase. To ensure stable and effective learning, particularly when dealing with complex tasks and potentially sparse rewards common in multimodal settings, we propose a novel Prioritized Advantage Distillation (PAD) to improve gradient quality by addressing specific GRPO limitations.

#### 4.1.1 PRIORITIZED ADVANTAGE DISTILLATION (PAD)

During multimodal RL training, we discover a significant challenge when applying GRPO in complex multimodal settings is “Gradient Stagnation”. This phenomenon refers to a reduction in learning efficacy due to a predominance of near-zero advantage estimates, which is particularly acute when dealing with sparse binary rewards. Essentially, if entire groups of generated responses yield uniform rewards (e.g., all correct or all incorrect), the resulting advantage signals become null, leading to zero policy gradients and thereby halting learning for those samples. This issue, also noted in concurrent works (Wang et al., 2025; Yu et al., 2025), can severely impede training progress. To specifically counteract gradient stagnation and enhance the efficiency of GRPO, we introduce Prioritized Advantage Distillation (PAD). PAD refines the training process by strategically focusing updates on the most informative samples within each batch, namely those exhibiting significant, non-zero advantage signals. The PAD mechanism, detailed below, operates on each batch after initial advantage estimation. It mainly contains the following three parts:

- **Per-Sequence Advantage Calculation:** Compute the absolute advantage  $|\hat{A}_i|$  for each sequence  $i$  in the original batch  $\mathcal{B}$ , representing its learning signal magnitude.
- **Effective Sample Filtering:** Form an “effective set”  $\mathcal{E}$  by selecting sequences  $i$  whose absolute advantage  $|\hat{A}_i|$  falls within a specified informative range  $[T_{low}, T_{high}]$ . Critically,  $T_{low} > 0$  filters out stagnant (near-zero advantage) samples, ensuring that candidates for sub-sampling provide potentially useful learning signals.
- **Prioritized Sub-sampling from Effective Set:** From this effective set  $\mathcal{E}$ ,  $k' = \min(\rho|\mathcal{B}|, |\mathcal{E}|)$  sequences are drawn to form a distilled mini-batch. Selection is prioritized based on sequences’ absolute advantages ( $\hat{A}_i$  for  $i \in \mathcal{E}$ ), with the probability for selecting sequence  $i$  determined by a temperature-controlled Softmax distribution:

$$\Pr(i \text{ is selected} \mid i \in \mathcal{E}) = \frac{\exp(\hat{A}_i/\tau)}{\sum_{j \in \mathcal{E}} \exp(\hat{A}_j/\tau)} \quad (4)$$

The temperature  $\tau$  governs sampling concentration and is typically decayed during training (e.g., linearly from 1.0 to 0.3) to shift from exploration towards exploitation. This enriches the mini-batch with the most informative samples from  $\mathcal{E}$ .

PAD thus directly counteracts gradient stagnation via a dual mechanism: first, by filtering out stagnant samples, and second, by prioritizing updates using informative, non-zero advantages from the

270 remaining set. This selective optimization of the learning process ensures efficient computational  
 271 resource allocation towards high-value samples. Consequently, PAD leads to enhanced training sta-  
 272 bility, improved learning efficiency, and more effective acquisition of complex reasoning skills.  
 273

274 **4.2 STAGE 2: TEXTUAL RL**  
 275

276 While MRL is indispensable for grounding reasoning across visual and textual inputs, intensive  
 277 MRL training can inadvertently lead to a decline in purely textual capabilities. To further elevate the  
 278 model’s capacity for sophisticated abstract reasoning, we integrate a subsequent Textual Reinforce-  
 279 ment Learning (TRL) phase. This stage aims to achieve both robust linguistic fluency and advanced  
 280 reasoning. Linguistic fluency is restored and enhanced by fine-tuning on high-quality, text-only  
 281 corpora focused on instruction-following and conversational abilities. Simultaneously, to foster ad-  
 282 vanced reasoning, the TRL phase exposes the model to complex, text-centric problem-solving tasks.  
 283 This compels the model to refine and generalize intricate reasoning patterns, articulate multi-step  
 284 thought processes with greater clarity, and master linguistic nuances essential for higher-order cog-  
 285 nition. For policy optimization during this TRL phase, we employ GRPO, augmented with our  
 286 proposed PAD mechanism for efficient sample utilization.  
 287

288 **5 EXPERIMENTS**

289 **5.1 EXPERIMENTS SETUP**  
 290

291 **Benchmarks** To comprehensively evaluate our model’s performance, we selected a diverse suite  
 292 of benchmarks targeting a wide range of reasoning abilities. The evaluation suite is organized by  
 293 domain: (1) Multimodal mathematical reasoning, assessed using MathVerse (Zhang et al., 2024b),  
 294 MathVision (Wang et al., 2024a), MathVista (Lu et al., 2023a), DynaMath (Zou et al., 2025), and  
 295 WeMath (Qiao et al., 2024b); (2) General multimodal reasoning, evaluated with LogicVista (Xiao  
 296 et al., 2024), MMMU (Yue et al., 2024a), MMMU-Pro (Yue et al., 2024b), CMMMU (Zhang et al.,  
 297 2024a), and MMStar Chen et al. (2024); and (3) Text-based reasoning, measured on challenging  
 298 mathematical benchmarks like AIME24/25 (Li et al., 2024) and MATH-500 (Hendrycks et al., 2021),  
 299 as well as general reasoning benchmarks such as GPQA (Rein et al., 2024) and MMLU Pro (Wang  
 300 et al., 2024b). Performance is reported as pass@1 accuracy for all benchmarks, with the exception  
 301 of AIME24/25, for which we use average@32 accuracy.  
 302

303 **Baselines** As shown in Table 2, baselines include: (1) leading closed-source models doubaol-1.5-  
 304 vision-pro-32k (Guo et al., 2025b), OpenAI-GPT-4o (Hurst et al., 2024), Claude-3.7-Sonnet (An-  
 305 thropic, 2024), Gemini-2.0-Flash (Gemini Team et al., 2023). (2) open-source general-purpose  
 306 MLLM Qwen2.5-VL-7B (Bai et al., 2025); and 3) specialized open-source reasoning MLLMs  
 307 VLAA-Thinker-7B (Chen et al., 2025a), OpenVLThinker-7B (Deng et al., 2025), MMR1-Math-v0  
 308 (Leng et al., 2025), MM-Eureka (Meng et al., 2025a), and VL-Rethinker-7B (Wang et al., 2025).  
 309

310 **5.2 IMPLEMENTATION DETAILS**  
 311

312 Our ReVisual-R1 models are based on the Qwen-2.5-VL-7B-Instruct and Qwen-2.5-VL-3B-Instruct  
 313 models. Its training comprised three distinct stages. The process begins with a cold-start phase  
 314 utilizing LLaMA Factory (Zheng et al., 2024) and pure text data to establish foundational language  
 315 understanding. Following this, Multimodal Reinforcement Learning (MRL) is implemented using  
 316 Easy R1 (Zheng et al., 2025). In this stage, the GRPO Kullback-Leibler (KL) divergence constraint  
 317 is omitted to encourage broader policy exploration. The final stage TRL is also conducted via Easy  
 318 R1. During TRL, the vision tower is frozen to concentrate learning on textual reasoning, and a  
 319 small KL penalty is incorporated alongside entropy annealing to enhance training stability. All  
 320 experiments are conducted on a setup of 8 NVIDIA A100-80G GPUs. Detailed prompt settings and  
 321 training hyperparameters are provided in the Appendix.  
 322

323 **5.3 TRAINING DATASETS**  
 324

325 The training of ReVisual-R1 follows our proposed three-stage methodology, utilizing carefully cu-  
 326 rated datasets for each phase. The cold-start phase employed approximately 283k pure text entries  
 327

**Table 2:** Performance comparison on diverse benchmarks. The best scores are **bold**; the second best are underlined (among open-source models). Scores in *italics* indicate that they are not reported in the original work and are obtained using the VLMEvalKit (Duan et al., 2024) for evaluation. AIME24 and AIME25 results are averaged over eight independent inference runs to reduce score variance. **MathVerse-V**, **DynaMath-W** and **WeMath-S** denotes the vision-only, worst, and strict settings, respectively.  $\Delta$  (e.g., **Ours-Open 3B Best**) denotes the improvement margin of the corresponding **ReVisual-R1** model over the best-performing **open-source** baseline model in the same scale across the respective column.

Model	Multimodal Reasoning Benchmarks						Textual Reasoning Benchmarks				
	MathVerse-V	MathVision	MathVista	DynaMath-W	WeMath-S	LogicVista	AIME24	AIME25	GPQA	MATH500	Avg.
<i>ClosedSource</i>											
doubao-1.5-vision-pro-32k	64.7	51.5	78.6	44.9	64.2	65.7	26.7	20.0	56.1	85.2	55.8
OpenAIGPT4o	40.6	31.1	59.9	34.5	42.9	64.4	9.3	8.3	49.9	74.6	41.6
Claude3.7Sonnet	52.0	41.3	66.8	39.7	58.2	49.3	20.0	13.3	61.1	80.4	48.2
Gemini2.0Flash	43.6	47.8	70.4	42.1	47.4	52.3	33.3	36.7	35.4	69.0	47.8
<i>3B-scale MLLMs</i>											
Qwen2.5-VL-3B	<i>33.0</i>	22.7	<i>60.0</i>	9.0	17.9	28.8	<i>6.7</i>	0.0	22.2	57.2	25.8
FAST-3B	<i>44.0</i>	<i>26.8</i>	<i>63.8</i>	<i>15.4</i>	23.3	35.4	<i>6.7</i>	<i>3.3</i>	25.3	55.4	29.9
VLAA-Thinker-3B	36.4	24.4	61.0	<i>18.2</i>	<i>33.8</i>	<i>38.5</i>	3.3	0.0	<i>27.8</i>	<i>61.4</i>	30.5
<b>ReVisual-R1-3B</b>	<b>46.2</b>	<b>46.0</b>	<b>64.8</b>	<b>24.6</b>	<b>39.6</b>	<b>45.4</b>	<b>40.0</b>	<b>36.7</b>	<b>37.4</b>	<b>84.2</b>	<b>46.5</b>
$\Delta$ ( <b>Ours-Open 3B Best</b> )	+2.2	+19.2	+1.0	+6.4	+5.8	+6.9	+33.3	+33.4	+9.6	+22.8	+16.0
<i>7B-scale Models</i>											
Qwen2.5VL7B	38.7	26.6	68.2	12.6	24.5	35.6	<i>10.0</i>	6.7	32.8	<i>67.2</i>	32.3
OpenVLThinker7B	<i>38.1</i>	25.9	72.3	<i>16.8</i>	35.2	44.5	5.0	1.7	28.3	<i>51.0</i>	31.9
MM-Eureka-Qwen-7B	<i>45.4</i>	26.9	73.0	<i>23.0</i>	21.8	46.3	6.7	3.3	34.3	66.6	34.7
MMR1-Math-v0	45.1	<i>30.2</i>	71.0	<i>17.4</i>	30.2	<i>50.8</i>	5.4	0.8	19.2	65.8	33.6
ThinkLite7BVL	42.9	24.6	71.6	16.5	<i>41.8</i>	42.7	8.8	<i>27.9</i>	24.8	<i>61.4</i>	36.3
VLAA-Thinker-7B	<i>48.2</i>	26.4	68.0	22.4	41.5	48.5	0.8	<i>12.6</i>	30.8	30.8	33.0
VL-Rethinker-7B	46.4	28.4	<i>73.7</i>	17.8	36.3	42.7	2.9	2.9	<i>37.4</i>	47.0	33.6
<b>ReVisual-R1-7B</b>	<b>53.6</b>	<b>48.8</b>	<b>73.1</b>	<b>27.5</b>	<b>42.0</b>	<b>52.3</b>	<b>53.3</b>	<b>43.3</b>	<b>47.5</b>	<b>89.2</b>	<b>53.1</b>
$\Delta$ ( <b>Ours-Open 7B Best</b> )	+5.4	+18.6	-0.6	+4.5	+0.2	+1.5	+43.3	+15.4	+10.1	+22.0	+16.8

focused on establishing foundational language understanding. Subsequently, the Multimodal Reinforcement Learning (MRL) phase used approximately 26k diverse multimodal entries from our GRAMMAR dataset to develop multimodal reasoning. Finally, the TRL phase consists of approximately 30k text entries designed to refine nuanced understanding and generation capabilities.

## 5.4 MAIN RESULTS

As shown in Table 2, our model demonstrates superior performance on math-related benchmarks compared to other open-source reasoning models and even outperforms some commercial MLLMs.

Specifically, on the 7B model scale, ReVisual-R1-7B achieves an impressive average score of 53.1%, a significant improvement of +16.8 percentage points over the baselines in Table 2 on textual and multimodal benchmarks. Notably, ReVisual-R1 secures the top position among open-source contenders in nine out of ten individual benchmarks: MathVerse (+5.4%  $\Delta$ ), MathVision (+18.6%  $\Delta$ ), DynaMath (+4.5%  $\Delta$ ), WeMath (+0.2%  $\Delta$ ), LogicVista (+1.5%  $\Delta$ ), AIME24 (+43.3%  $\Delta$ ), AIME25 (+15.4%  $\Delta$ ), GPQA (+10.1%  $\Delta$ ), and MATH500 (+22.0%  $\Delta$ ). All these results present the superior performance of our ReVisual-R1 on both multimodal benchmarks as well as textual benchmarks.

When compared to closed-source commercial models, ReVisual-R1 also exhibits highly competitive performance. For instance, its average score (53.1%) surpasses that of OpenAI-GPT-4o (41.6%). On specific demanding benchmarks such as MATH500, ReVisual-R1 (89.2%) outperforms both douba-1.5-vision-pro-32k (85.2%) and OpenAI-GPT-4o (74.6%). Similarly, on AIME24 and AIME25, ReVisual-R1 demonstrates substantial leads over these commercial offerings. While some closed-source models like douba-1.5-vision-pro-32k show a higher overall average (55.8%), ReVisual-R1's ability to outperform them on several key reasoning tasks highlights its specialized strengths.

To further demonstrate the effectiveness of our training framework, we conduct experiments on 3B model scale, leading to ReVisual-R1-3B. As demonstrated in Table 2, our model also demonstrates superior performance on this model size. Specifically, our model outperforms VLAA-Thinker-3B

378 **Table 3:** Ablation study of different training stage combinations applied to the ReVisual-R1 model, building  
 379 upon a Cold Start. Best results per column are **bold** and second-best are underlined. Mixed-RL denotes that  
 380 the model is jointly optimized with both MRL and TRL objectives in a mixed training stage.

Training Strategies	MathVerse-V	MathVision	MathVista	DynaMath-W	WeMath-S	LogicVista	Avg
Cold Start (CS) only	<u>51.9</u>	47.9	70.5	<u>26.5</u>	35.8	50.1	47.1
CS + MRL	50.9	47.6	<u>71.9</u>	25.7	<u>38.8</u>	<u>51.2</u>	<u>47.7</u>
CS + TRL	47.3	47.3	71.0	25.2	33.7	44.7	44.9
<b>CS + MRL + TRL</b>	<b>53.6</b>	<b>48.8</b>	<b>73.1</b>	<b>27.5</b>	<b>42.0</b>	<b>52.3</b>	<b>49.6</b>
CS + TRL + MRL	47.5	<u>48.0</u>	70.3	24.2	35.0	48.2	45.5
CS + Mixed-RL	49.3	48.2	72.1	25.7	38.8	51.2	47.6

389 **Table 4:** Ablation results demonstrating the impact of Prioritized Advantage Distillation (PAD) and its core  
 390 components. Best results per column are **bold** and second-best are underlined.

Model Configuration	Strategy	MathVerse	MathVision	MathVista	DynaMath	WeMath	LogicVista	Avg
ReVisual-R1 (CS + MRL)	PAD	<b>50.9</b>	<b>47.6</b>	<b>71.9</b>	<u>25.7</u>	<b>38.8</b>	<b>51.2</b>	<b>47.7</b>
<i>w/o PAD Components:</i>								
- Full PAD (Baseline)	GRPO-Baseline	47.6	45.8	68.8	25.2	34.8	48.6	45.1
- No Prioritized Sub-sampling	GRPO-Filter	47.7	<u>46.7</u>	<u>71.2</u>	25.5	35.1	<u>49.7</u>	46.0
- No Effective Sample Filtering	Random-Sampling	<u>47.9</u>	46.4	70.7	<b>26.1</b>	<u>37.1</u>	49.3	<u>46.2</u>
Other Strategy	DAPO	48.3	46.3	69.2	25.4	38.3	49.2	46.1

399 across all benchmarks and obtains an average 16.0% improvement. These results further verify the  
 400 generalization of our ReVisual-R1.

401 Collectively, these results validate the efficacy of our proposed training method, including the struc-  
 402 tured three-stage curriculum and enhancements like Prioritized Advantage Distillation.

## 405 5.5 ABLATION STUDY

### 406 5.5.1 ABLATION ON SRO

408 To validate the effectiveness of our Staged Reinforcement Optimization (SRO) framework, we con-  
 409 duct ablation studies on different combinations of Multimodal RL (MRL) and Textual RL (TRL)  
 410 phases, all building upon our optimized text-centric cold-start (CS). As shown in Table 3, the empir-  
 411 ical results verify that our proposed CS + MRL + TRL (ReVisual-R1-MTR) sequence consistently  
 412 yields the highest average performance (49.6 Avg). This outcome affirms our core hypothesis: an  
 413 initial MRL phase establishes strong visual grounding, followed by a TRL phase to refine textual  
 414 fluency and abstract reasoning, is crucial for developing superior multimodal capabilities.

415 In a more detailed analysis, the CS + MRL only model (47.7 Avg), while performing well on visually  
 416 intensive tasks such as MathVista (71.9), does not reach the overall performance of the full MTR  
 417 sequence. This further highlights the importance of the subsequent TRL stage. The alternative SRO  
 418 ordering, CS + TRL + MRL (45.5 Avg), also proved less effective than our MTR approach. This  
 419 finding indicates that establishing strong visual grounding before intensive textual refinement allows  
 420 for more synergistic learning.

421 In addition, we perform a mixed-RL strategy to investigate the necessity of our staged reinforcement  
 422 learning. In this setting, we train the cold-start model on a mixture of multimodal and textual data.  
 423 However, as shown in Table 3, we observe that this mixed setting can only get an average 47.6 score,  
 424 which is significantly lower than the performance of our staged RL. It shows that our MRL-then-  
 425 TRL ordering within our SRO framework is a more effective strategy than simultaneously training  
 426 on mixed-modality data in the RLVR stage.

### 428 5.5.2 ABLATION STUDY ON PAD

430 In this section, we conduct ablation studies to verify the effectiveness of our proposed Prioritized  
 431 Advantage Distillation (PAD), examining its overall efficacy, the contribution of its components, and  
 432 its sensitivity to key hyperparameters.

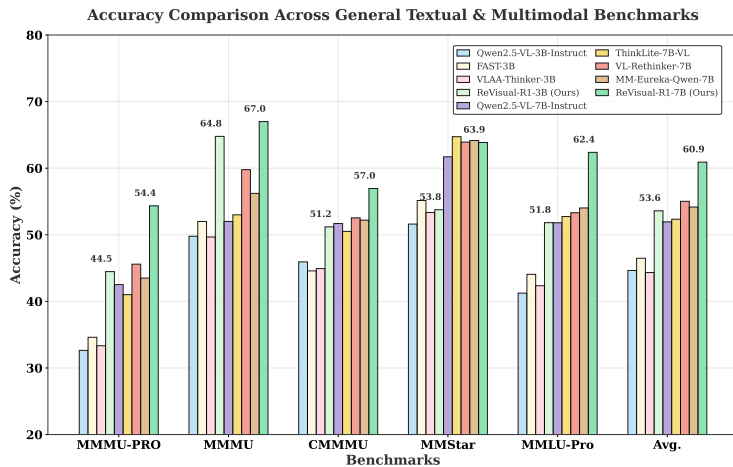


Figure 3: Performance comparison on general textual and multimodal benchmarks.  
Reward/Accuracy Comparison

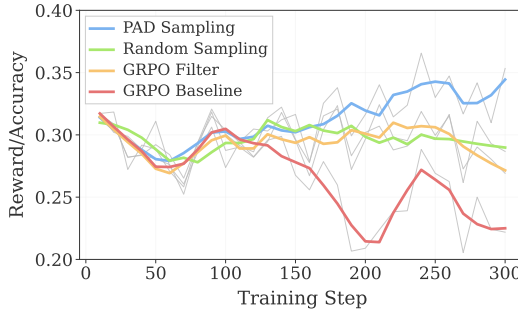


Figure 4: Ablation of training dynamics of our PAD.

To assess PAD’s impact, its full implementation is compared against GRPO-Baseline, GRPO-Filter-only, and Random-Sampling strategies. Table 4 demonstrates that full PAD achieved superior performance on mathematical reasoning benchmarks, highlighting the importance of its core components: effective sample filtering and prioritized sub-sampling. Meanwhile, we compare our method with DAPO and observe that our PAD can also present significantly better performance than DAPO. To further demonstrate the effectiveness of our Training dynamics (Figure 4) further corroborate PAD’s effectiveness, with its sampling strategy yielding higher reward accuracy and faster convergence.

### 5.5.3 GENERALIZATION OF REVISUAL-R1

To further evaluate the generalization capacity of our method, we test the model on several knowledge-intensive benchmarks, including MMMU, MMMU-Pro, and CMMU, as well as on general-purpose multimodal perception (MMStar) and textual understanding (MMLU). The results, presented in Figure 3, show that our method consistently performs superior across these benchmarks. The more detailed performance is shown in Table 6. It further indicates that the generality of our approach on general tasks and provides further evidence that textual reasoning capabilities can benefit on general multimodal and textual tasks.

## 6 RELATED WORK

### 6.1 MULTIMODAL LARGE LANGUAGE MODEL

Multimodal Large Language Model (MLLM) is a key research area. While leading closed-source models (e.g., GPT-o3 (OpenAI, 2025), Kimi-VL (Kimi Team, 2025)) excel at long Chain-of-Thought (CoT) reasoning, open-source contributions have focused on CoT adaptations (Liu et al., 2023; Guo et al., 2024; Su et al., 2024) and Supervised Fine-Tuning (SFT) with reasoning traces (Mitra et al., 2024b; Zhang et al., 2024c) (Gao et al., 2024). DeepSeek-R1 (Guo et al., 2025a) has further

486 spurred Reinforcement Learning (RL) applications for visual reasoning (Huang et al., 2025) (Dong  
 487 et al., 2024) and specialized domains like mathematical reasoning. Nevertheless, many MLLM rea-  
 488 soning models (Wang et al., 2025) (Deng et al., 2025) (Yang et al., 2025) (Chen et al., 2025b) are  
 489 limited by generating relatively short responses, which often curtail genuine reflection, thorough  
 490 visual exploration, and consequently, deep multimodal reasoning. Our work, in contrast, introduces  
 491 a novel framework to enable MLLMs to generate significantly longer, reflective responses, thereby  
 492 facilitating long CoT reasoning to unlock more comprehensive multimodal reasoning capabilities.

## 493 6.2 REINFORCEMENT LEARNING IN REASONING

494 Current LLM research explores direct RL fine-tuning, specialized cold-start datasets for long-form  
 495 reasoning, and advanced algorithms like Group Relative Policy Optimization (GRPO) (Shao et al.,  
 496 2024) and its refinements (e.g., DAPO (Yu et al., 2025), DR.GRPO (Liu et al., 2025), GPG (Chu  
 497 et al., 2025)) to elicit deeper reasoning. However, RL application to multimodal reasoning in  
 498 MLLMs is nascent. Initial MLLMs efforts focus on subdomains like math reasoning (Meng et al.,  
 499 2025b; Peng et al., 2025) or generative reward models (Gao et al., 2025), often utilizing data from  
 500 commercial models. Nonetheless, successes such as DeepSeek-R1’s (Guo et al., 2025a) rule-based  
 501 RL are spurring similar MLLMs investigations, indicating growing interest in RL for unlocking  
 502 sophisticated multimodal reasoning.

## 503 6.3 LIMITATIONS AND FUTURE WORK

504 Despite the strong empirical gains demonstrated by ReVisual-R1, our study has several limitations  
 505 that point toward crucial directions for future work. While we justify the efficacy of the optimized  
 506 cold start, staged multimodal and text-only RL, and PAD through substantial empirical gains and  
 507 ablations, we currently lack a rigorous theoretical foundation. Specifically, a deeper theoretical  
 508 account is needed to explain why these text-centric optimization strategies, such as the cold start,  
 509 effectively enhance model reasoning capabilities, and to provide a more principled explanation for  
 510 the staged RL methodology. Furthermore, our scalability evidence is limited to mid-sized models.  
 511 We demonstrated that training on complex, high-difficulty textual reasoning data transfers benefits  
 512 to both the textual and multimodal reasoning performance of 3B and 7B models. However, we  
 513 have not yet validated these advantages across larger-scale architectures, such as MoE models, or  
 514 generalized them to other foundational model families and larger size regimes. Finally, we will  
 515 systematically investigate the interplay between data type and training stage. We will extensively  
 516 explore the impact of the ratio and quality of multimodal versus textual data utilized during both the  
 517 cold start and RL phases. The ultimate goal of this exploration is to determine an optimal curriculum  
 518 recipe that jointly maximizes performance across diverse skill clusters, notably in STEM reasoning,  
 519 perceptual grounding, and general domains.

## 520 7 CONCLUSION

521 This paper introduces ReVisual-R1, a 3B and 7B open-source MLLM designed to address prevalent  
 522 challenges in cultivating sophisticated multimodal reasoning. By systematically integrating a strate-  
 523 gic, high-difficulty text-only cold-start phase for foundational reasoning, a Multimodal RL stage  
 524 employing GRPO stabilized by our novel Prioritized Advantage Distillation (PAD) mechanism, and  
 525 a final TextRL refinement phase, our structured three-stage curriculum demonstrates that thought-  
 526 ful data strategy and targeted algorithmic optimizations are pivotal. ReVisual-R1 achieves superior  
 527 performance among open-source 7B models on a suite of challenging multimodal, textual reasoning  
 528 and generalization benchmarks. This work underscores that careful curriculum design and algo-  
 529 rithmic enhancements, rather than sheer model scale, can unlock robust, self-reflective multimodal  
 530 reasoning.

540  
541

## REPRODUCIBILITY STATEMENT

542  
543  
544  
545

To ensure the reproducibility of our work, we provide an anonymous code repository in the supplementary materials containing the full implementation of our Revisual-R1 algorithm. All datasets used for training and evaluation are publicly available, and a comprehensive breakdown of our experimental setup, including all key hyperparameters, is detailed in Appendix.

546

## ETHICS STATEMENT

548

The development of our model, ReVisual-R1, and the curation of the GRAMMAR dataset were conducted with close attention to ethical guidelines. Our research is grounded in the use of publicly available and open-source academic datasets, which were rigorously filtered during the creation of GRAMMAR to ensure no personal, private, or sensitive information was included. The work does not involve human subjects, and its objective is to advance research in multimodal reasoning for the open-source community. We foresee no direct societal risks or harmful applications.

544

545  
546

## REFERENCES

547

Alon Albalak, Duy Phung, Nathan Lile, Rafael Rafailov, Kanishk Gandhi, Louis Castricato, Anikait Singh, Chase Blagden, Violet Xiang, Dakota Mahan, and Nick Haber. Big-math: A large-scale, high-quality math dataset for reinforcement learning in language models. *CoRR*, abs/2502.17387, 2025. doi: 10.48550/ARXIV.2502.17387. URL <https://doi.org/10.48550/arXiv.2502.17387>.

548  
549

Anthropic. Claude 3.7 sonnet. <https://www.anthropic.com>, 2024.

550  
551  
552  
553

Shuai Bai, Keqin Chen, Xuejing Liu, Jialin Wang, Wenbin Ge, Sibo Song, Kai Dang, Peng Wang, Shijie Wang, Jun Tang, et al. Qwen2. 5-vl technical report. *arXiv preprint arXiv:2502.13923*, 2025.

554  
555  
556  
557

Ricardo JGB Campello, Davoud Moulavi, and Jörg Sander. Density-based clustering based on hierarchical density estimates. In *Pacific-Asia conference on knowledge discovery and data mining*, pp. 160–172. Springer, 2013.

558  
559  
560  
561

Hardy Chen, Haoqin Tu, Fali Wang, Hui Liu, Xianfeng Tang, Xinya Du, Yuyin Zhou, and Cihang Xie. Sft or rl? an early investigation into training rl-like reasoning large vision-language models. *arXiv preprint arXiv:2504.11468*, 2025a.

562  
563  
564  
565  
566

Jiaqi Chen, Jianheng Tang, Jinghui Qin, Xiaodan Liang, Lingbo Liu, Eric P. Xing, and Liang Lin. Geoqa: A geometric question answering benchmark towards multimodal numerical reasoning. In Chengqing Zong, Fei Xia, Wenjie Li, and Roberto Navigli (eds.), *Findings of the Association for Computational Linguistics: ACL/IJCNLP 2021, Online Event, August 1-6, 2021*, volume ACL/IJCNLP 2021 of *Findings of ACL*, pp. 513–523. Association for Computational Linguistics, 2021. doi: 10.18653/V1/2021.FINDINGS-ACL.46. URL <https://doi.org/10.18653/v1/2021.findings-acl.46>.

567

Jiaqi Chen, Tong Li, Jinghui Qin, Pan Lu, Liang Lin, Chongyu Chen, and Xiaodan Liang. Unigeo: Unifying geometry logical reasoning via reformulating mathematical expression. In Yoav Goldberg, Zornitsa Kozareva, and Yue Zhang (eds.), *Proceedings of the 2022 Conference on Empirical Methods in Natural Language Processing, EMNLP 2022, Abu Dhabi, United Arab Emirates, December 7-11, 2022*, pp. 3313–3323. Association for Computational Linguistics, 2022. doi: 10.18653/V1/2022.EMNLP-MAIN.218. URL <https://doi.org/10.18653/v1/2022.emnlp-main.218>.

568  
569  
570  
571  
572  
573

Liang Chen, Lei Li, Haozhe Zhao, Yifan Song, and Vinci. R1-v: Reinforcing super generalization ability in vision-language models with less than \$3. <https://github.com/Deep-Agent/R1-V>, 2025b. Accessed: 2025-02-02.

574

Lin Chen, Jinsong Li, Xiaoyi Dong, Pan Zhang, Yuhang Zang, Zehui Chen, Haodong Duan, Jiaqi Wang, Yu Qiao, Dahua Lin, et al. Are we on the right way for evaluating large vision-language models? *arXiv preprint arXiv:2403.20330*, 2024.

594 Xiangxiang Chu, Hailang Huang, Xiao Zhang, Fei Wei, and Yong Wang. Gpg: A simple and  
 595 strong reinforcement learning baseline for model reasoning, 2025. URL <https://arxiv.org/abs/2504.02546>.

596

597 Yihe Deng, Hritik Bansal, Fan Yin, Nanyun Peng, Wei Wang, and Kai-Wei Chang. Openvlthinker:  
 598 An early exploration to complex vision-language reasoning via iterative self-improvement, 2025.  
 599 URL <https://arxiv.org/abs/2503.17352>.

600

601 Yuhao Dong, Zuyan Liu, Hai-Long Sun, Jingkang Yang, Winston Hu, Yongming Rao, and Ziwei  
 602 Liu. Insight-v: Exploring long-chain visual reasoning with multimodal large language models.  
 603 *arXiv preprint arXiv:2411.14432*, 2024.

604

605 Haodong Duan, Junming Yang, Yuxuan Qiao, Xinyu Fang, Lin Chen, Yuan Liu, Xiaoyi Dong,  
 606 Yuhang Zang, Pan Zhang, Jiaqi Wang, Dahua Lin, and Kai Chen. Vlmevalkit: An open-  
 607 source toolkit for evaluating large multi-modality models. In Jianfei Cai, Mohan S. Kankanhalli,  
 608 Balakrishnan Prabhakaran, Susanne Boll, Ramanathan Subramanian, Liang Zheng, Vivek K.  
 609 Singh, Pablo César, Lexing Xie, and Dong Xu (eds.), *Proceedings of the 32nd ACM Inter-  
 610 national Conference on Multimedia, MM 2024, Melbourne, VIC, Australia, 28 October 2024  
 611 - 1 November 2024*, pp. 11198–11201. ACM, 2024. doi: 10.1145/3664647.3685520. URL  
<https://doi.org/10.1145/3664647.3685520>.

612

613 Hugging Face. Open r1: A fully open reproduction of deepseek-r1, January 2025. URL <https://github.com/huggingface/open-r1>.

614

615 Minghe Gao, Shuang Chen, Liang Pang, Yuan Yao, Jisheng Dang, Wenqiao Zhang, Juncheng Li,  
 616 Siliang Tang, Yueling Zhuang, and Tat-Seng Chua. Fact :teaching mllms with faithful, concise  
 617 and transferable rationales, 2024. URL <https://arxiv.org/abs/2404.11129>.

618

619 Minghe Gao, Xuqi Liu, Zhongqi Yue, Yang Wu, Shuang Chen, Juncheng Li, Siliang Tang, Fei Wu,  
 620 Tat-Seng Chua, and Yueling Zhuang. Benchmarking multimodal cot reward model stepwise by  
 621 visual program, 2025. URL <https://arxiv.org/abs/2504.06606>.

622

623 Gemini Team, Rohan Anil, Sebastian Borgeaud, Jean-Baptiste Alayrac, Jiahui Yu, Radu Soricut,  
 624 Johan Schalkwyk, Andrew M Dai, Anja Hauth, Katie Millican, et al. Gemini: a family of highly  
 625 capable multimodal models. *arXiv preprint arXiv:2312.11805*, 2023.

626

627 Daya Guo, Dejian Yang, Haowei Zhang, Junxiao Song, Ruoyu Zhang, Runxin Xu, Qihao Zhu,  
 628 Shirong Ma, Peiyi Wang, Xiao Bi, et al. Deepseek-r1: Incentivizing reasoning capability in llms  
 629 via reinforcement learning. *arXiv preprint arXiv:2501.12948*, 2025a.

630

631 Dong Guo, Faming Wu, Feida Zhu, Fuxing Leng, Guang Shi, Haobin Chen, Haoqi Fan, Jian Wang,  
 632 Jianyu Jiang, Jiawei Wang, et al. Seed1. 5-vl technical report. *arXiv preprint arXiv:2505.07062*,  
 633 2025b.

634

635 Jarvis Guo, Tuney Zheng, Yuelin Bai, Bo Li, Yubo Wang, King Zhu, Yizhi Li, Graham Neubig,  
 636 Wenhui Chen, and Xiang Yue. Mammoth-vl: Eliciting multimodal reasoning with instruction  
 637 tuning at scale, 2024. URL <https://arxiv.org/abs/2412.05237>.

638

639 Zhiwei He, Tian Liang, Jiahao Xu, Qiuzhi Liu, Xingyu Chen, Yue Wang, Linfeng Song, Dian Yu,  
 640 Zhenwen Liang, Wenxuan Wang, Zhusong Zhang, Rui Wang, Zhaopeng Tu, Haitao Mi, and  
 641 Dong Yu. Deepmath-103k: A large-scale, challenging, decontaminated, and verifiable mathemat-  
 642 ical dataset for advancing reasoning, 2025. URL <https://arxiv.org/abs/2504.11456>.

643

644 Dan Hendrycks, Collin Burns, Saurav Kadavath, Akul Arora, Steven Basart, Eric Tang, Dawn Song,  
 645 and Jacob Steinhardt. Measuring mathematical problem solving with the math dataset. *arXiv  
 646 preprint arXiv:2103.03874*, 2021.

647

648 Wenzuan Huang, Bohan Jia, Zijie Zhai, Shaosheng Cao, Zheyu Ye, Fei Zhao, Yao Hu, and Shaohui  
 649 Lin. Vision-r1: Incentivizing reasoning capability in multimodal large language models. *arXiv  
 650 preprint arXiv:2503.06749*, 2025.

651

652 Aaron Hurst, Adam Lerer, Adam P Goucher, Adam Perelman, Aditya Ramesh, Aidan Clark, AJ Os-  
 653 trow, Akila Welihinda, Alan Hayes, Alec Radford, et al. Gpt-4o system card. *arXiv preprint  
 654 arXiv:2410.21276*, 2024.

648 Samira Ebrahimi Kahou, Vincent Michalski, Adam Atkinson, Ákos Kádár, Adam Trischler, and  
 649 Yoshua Bengio. Figureqa: An annotated figure dataset for visual reasoning. In *6th International*  
 650 *Conference on Learning Representations, ICLR 2018, Vancouver, BC, Canada, April 30 - May*  
 651 *3, 2018, Workshop Track Proceedings*. OpenReview.net, 2018. URL <https://openreview.net/forum?id=H1mz0OyDz>.

652

653 Kimi Team. Kimi k1. 5: Scaling reinforcement learning with llms. *arXiv preprint arXiv:2501.12599*,  
 654 2025.

655

656 Chankyu Lee, Rajarshi Roy, Mengyao Xu, Jonathan Raiman, Mohammad Shoeybi, Bryan Catan-  
 657 zaro, and Wei Ping. Nv-embed: Improved techniques for training llms as generalist embedding  
 658 models. *arXiv preprint arXiv:2405.17428*, 2024.

659

660 Sicong Leng, Jing Wang, Jiaxi Li, Hao Zhang, Zhiqiang Hu, Boqiang Zhang, Hang Zhang, Yuming  
 661 Jiang, Xin Li, Deli Zhao, Fan Wang, Yu Rong, Aixin Sun, and Shijian Lu. Mmr1: Advancing the  
 662 frontiers of multimodal reasoning. <https://github.com/LengSicong/MMR1>, 2025.

663

664 Jia Li, Edward Beeching, Lewis Tunstall, Ben Lipkin, Roman Soletskyi, Shengyi Huang, Kashif  
 665 Rasul, Longhui Yu, Albert Q. Jiang, Ziju Shen, et al. Numinamath: The largest public  
 666 dataset in ai4maths with 860k pairs of competition math problems and solutions. <https://huggingface.co/datasets/Numinamath>, 2024. Hugging Face repository, 13:9.

667

668 Jia LI, Edward Beeching, Lewis Tunstall, Ben Lipkin, Roman Soletskyi, Shengyi Costa Huang,  
 669 Kashif Rasul, Longhui Yu, Albert Jiang, Ziju Shen, Zihan Qin, Bin Dong, Li Zhou, Yann  
 670 Fleureau, Guillaume Lample, and Stanislas Polu. Numinamath. [<https://huggingface.co/AI-MO/NuminaMath-CoT>] ([https://github.com/project-numina/aimo-progress-prize/blob/main/report/numina\\_dataset.pdf](https://github.com/project-numina/aimo-progress-prize/blob/main/report/numina_dataset.pdf)), 2024.

671

672 Zhuowan Li, Xingrui Wang, Elias Stengel-Eskin, Adam Kortylewski, Wufei Ma, Benjamin Van  
 673 Durme, and Alan L. Yuille. Super-clevr: A virtual benchmark to diagnose domain robust-  
 674 ness in visual reasoning. In *IEEE/CVF Conference on Computer Vision and Pattern Recog-  
 675 nition, CVPR 2023, Vancouver, BC, Canada, June 17-24, 2023*, pp. 14963–14973. IEEE, 2023.  
 676 doi: 10.1109/CVPR52729.2023.01437. URL <https://doi.org/10.1109/CVPR52729.2023.01437>.

677

678

679 Haotian Liu, Chunyuan Li, Qingyang Wu, and Yong Jae Lee. Visual instruction tuning, 2023. URL  
 680 <https://arxiv.org/abs/2304.08485>.

681

682 Zichen Liu, Changyu Chen, Wenjun Li, Penghui Qi, Tianyu Pang, Chao Du, Wee Sun Lee, and Min  
 683 Lin. Understanding r1-zero-like training: A critical perspective. *arXiv preprint arXiv:2503.20783*,  
 2025.

684

685 Pan Lu, Ran Gong, Shibiao Jiang, Liang Qiu, Siyuan Huang, Xiaodan Liang, and Song-Chun Zhu.  
 686 Inter-gps: Interpretable geometry problem solving with formal language and symbolic reasoning.  
 687 In Chengqing Zong, Fei Xia, Wenjie Li, and Roberto Navigli (eds.), *Proceedings of the 59th An-  
 688 nual Meeting of the Association for Computational Linguistics and the 11th International Joint  
 689 Conference on Natural Language Processing, ACL/IJCNLP 2021, (Volume 1: Long Papers), Vir-  
 690 tual Event, August 1-6, 2021*, pp. 6774–6786. Association for Computational Linguistics, 2021a.  
 691 doi: 10.18653/V1/2021.ACL-LONG.528. URL <https://doi.org/10.18653/v1/2021.acl-long.528>.

692

693 Pan Lu, Liang Qiu, Jiaqi Chen, Tanglin Xia, Yizhou Zhao, Wei Zhang, Zhou Yu, Xiaodan  
 694 Liang, and Song-Chun Zhu. Iconqa: A new benchmark for abstract diagram under-  
 695 standing and visual language reasoning. In Joaquin Vanschoren and Sai-Kit Yeung (eds.),  
 696 *Proceedings of the Neural Information Processing Systems Track on Datasets and Bench-  
 697 marks 1, NeurIPS Datasets and Benchmarks 2021, December 2021, virtual*, 2021b. URL  
 698 <https://datasets-benchmarks-proceedings.neurips.cc/paper/2021/hash/d3d9446802a44259755d38e6d163e820-Abstract-round2.html>.

699

700 Pan Lu, Hritik Bansal, Tony Xia, Jiacheng Liu, Chunyuan Li, Hannaneh Hajishirzi, Hao Cheng, Kai-  
 701 Wei Chang, Michel Galley, and Jianfeng Gao. Mathvista: Evaluating mathematical reasoning of  
 foundation models in visual contexts. *arXiv preprint arXiv:2310.02255*, 2023a.

702 Pan Lu, Liang Qiu, Kai-Wei Chang, Ying Nian Wu, Song-Chun Zhu, Tanmay Rajpurohit, Peter  
 703 Clark, and Ashwin Kalyan. Dynamic prompt learning via policy gradient for semi-structured  
 704 mathematical reasoning. In *The Eleventh International Conference on Learning Representations, ICLR 2023, Kigali, Rwanda, May 1-5, 2023*. OpenReview.net, 2023b. URL <https://openreview.net/forum?id=DHyHRBwJUTN>.

707 Fanqing Meng, Lingxiao Du, Zongkai Liu, Zhixiang Zhou, Quanfeng Lu, Daocheng Fu, Botian Shi,  
 708 Wenhui Wang, Junjun He, Kaipeng Zhang, Ping Luo, Yu Qiao, Qiaosheng Zhang, and Wenqi Shao.  
 709 Mm-eureka: Exploring visual aha moment with rule-based large-scale reinforcement learning.  
 710 *CoRR*, abs/2503.07365, 2025a. doi: 10.48550/ARXIV.2503.07365. URL <https://doi.org/10.48550/arXiv.2503.07365>.

712 Fanqing Meng, Lingxiao Du, Zongkai Liu, Zhixiang Zhou, Quanfeng Lu, Daocheng Fu, Botian Shi,  
 713 Wenhui Wang, Junjun He, Kaipeng Zhang, et al. Mm-eureka: Exploring visual aha moment with  
 714 rule-based large-scale reinforcement learning. *arXiv preprint arXiv:2503.07365*, 2025b.

716 Arindam Mitra, Hamed Khanpour, Corby Rosset, and Ahmed Awadallah. Orca-math: Unlocking  
 717 the potential of slms in grade school math. *CoRR*, abs/2402.14830, 2024a. doi: 10.48550/ARXIV.  
 718 2402.14830. URL <https://doi.org/10.48550/arXiv.2402.14830>.

719 Chancharik Mitra, Brandon Huang, Trevor Darrell, and Roei Herzig. Compositional chain-of-  
 720 thought prompting for large multimodal models, 2024b. URL <https://arxiv.org/abs/2311.17076>.

723 Ivan Moshkov, Darragh Hanley, Ivan Sorokin, Shubham Toshniwal, Christof Henkel, Benedikt  
 724 Schifferer, Wei Du, and Igor Gitman. Aimo-2 winning solution: Building state-of-the-art math-  
 725 ematical reasoning models with openmathreasoning dataset. *arXiv preprint arXiv:2504.16891*,  
 726 2025.

727 Niklas Muennighoff, Zitong Yang, Weijia Shi, Xiang Lisa Li, Li Fei-Fei, Hannaneh Hajishirzi, Luke  
 728 Zettlemoyer, Percy Liang, Emmanuel Candès, and Tatsunori Hashimoto. s1: Simple test-time  
 729 scaling, 2025. URL <https://arxiv.org/abs/2501.19393>.

730 OpenAI. Introduction to chatgpt-o3, 2025. URL <https://openai.com/index/introducing-o3-and-o4-mini/>.

733 Shuai Peng, Di Fu, Liangcai Gao, Xiuqin Zhong, Hongguang Fu, and Zhi Tang. Multimath: Bridg-  
 734 ing visual and mathematical reasoning for large language models. *CoRR*, abs/2409.00147, 2024.  
 735 doi: 10.48550/ARXIV.2409.00147. URL <https://doi.org/10.48550/arXiv.2409.00147>.

737 Yingzhe Peng, Gongrui Zhang, Miaozen Zhang, Zhiyuan You, Jie Liu, Qipeng Zhu, Kai Yang,  
 738 Xingzhong Xu, Xin Geng, and Xu Yang. Lmm-r1: Empowering 3b lmms with strong reasoning  
 739 abilities through two-stage rule-based rl. *arXiv preprint arXiv:2503.07536*, 2025.

741 Runqi Qiao, Qiuna Tan, Guanting Dong, Minhui Wu, Chong Sun, Xiaoshuai Song, Zhuoma  
 742 GongQue, Shanglin Lei, Zhe Wei, MiaoXuan Zhang, Runfeng Qiao, Yifan Zhang, Xiao Zong,  
 743 Yida Xu, Muxi Diao, Zhimin Bao, Chen Li, and Honggang Zhang. We-math: Does your  
 744 large multimodal model achieve human-like mathematical reasoning?, 2024a. URL <https://arxiv.org/abs/2407.01284>.

746 Runqi Qiao, Qiuna Tan, Guanting Dong, Minhui Wu, Chong Sun, Xiaoshuai Song, Zhuoma  
 747 GongQue, Shanglin Lei, Zhe Wei, MiaoXuan Zhang, et al. We-math: Does your large multi-  
 748 modal model achieve human-like mathematical reasoning? *arXiv preprint arXiv:2407.01284*,  
 749 2024b.

750 David Rein, Betty Li Hou, Asa Cooper Stickland, Jackson Petty, Richard Yuanzhe Pang, Julien Di-  
 751 rani, Julian Michael, and Samuel R Bowman. Gpqa: A graduate-level google-proof q&a bench-  
 752 mark. In *First Conference on Language Modeling*, 2024.

754 ByteDance Seed, Jiaze Chen, Tiantian Fan, Xin Liu, Lingjun Liu, Zhiqi Lin, Mingxuan Wang,  
 755 Chengyi Wang, Xiangpeng Wei, Wenyuan Xu, et al. Seed1. 5-thinking: Advancing superb rea-  
 soning models with reinforcement learning. *arXiv e-prints*, pp. arXiv–2504, 2025.

756 Zhihong Shao, Peiyi Wang, Qihao Zhu, Runxin Xu, Junxiao Song, Xiao Bi, Haowei Zhang,  
 757 Mingchuan Zhang, YK Li, Y Wu, et al. Deepseekmath: Pushing the limits of mathematical  
 758 reasoning in open language models. *arXiv preprint arXiv:2402.03300*, 2024.

759

760 Zhaochen Su, Jun Zhang, Tong Zhu, Xiaoye Qu, Juntao Li, Min Zhang, and Yu Cheng. Timo:  
 761 Towards better temporal reasoning for language models. *arXiv preprint arXiv:2406.14192*, 2024.

762

763 OpenThoughts Team. Open Thoughts. <https://open-thoughts.ai>, January 2025.

764

765 Haozhe Wang, Chao Qu, Zuming Huang, Wei Chu, Fangzhen Lin, and Wenhua Chen. Vl-rethinker:  
 766 Incentivizing self-reflection of vision-language models with reinforcement learning. *arXiv  
 767 preprint arXiv:2504.08837*, 2025.

768

769 Ke Wang, Junting Pan, Weikang Shi, Zimu Lu, Houxing Ren, Aojun Zhou, Mingjie Zhan, and Hong-  
 770 sheng Li. Measuring multimodal mathematical reasoning with math-vision dataset. *Advances in  
 771 Neural Information Processing Systems*, 37:95095–95169, 2024a.

772

773 Yubo Wang, Xueguang Ma, Ge Zhang, Yuansheng Ni, Abhranil Chandra, Shiguang Guo, Weiming  
 774 Ren, Aaran Arulraj, Xuan He, Ziyan Jiang, et al. Mmlu-pro: A more robust and challenging multi-  
 775 task language understanding benchmark. *Advances in Neural Information Processing Systems*, 37:  
 776 95266–95290, 2024b.

777

778 Peng Xia, Kangyu Zhu, Haoran Li, Tianze Wang, Weijia Shi, Sheng Wang, Linjun Zhang, James  
 779 Zou, and Huaxiu Yao. Mmed-rag: Versatile multimodal rag system for medical vision language  
 780 models. In *The Thirteen International Conference on Learning Representations*.

781

782 Yijia Xiao, Edward Sun, Tianyu Liu, and Wei Wang. Logicvista: Multimodal llm logical reasoning  
 783 benchmark in visual contexts, 2024. URL <https://arxiv.org/abs/2407.04973>.

784

785 Jianhao Yan, Yafu Li, Zican Hu, Zhi Wang, Ganqu Cui, Xiaoye Qu, Yu Cheng, and Yue Zhang.  
 786 Learning to reason under off-policy guidance. *arXiv preprint arXiv:2504.14945*, 2025.

787

788 Yi Yang, Xiaoxuan He, Hongkun Pan, Xiyan Jiang, Yan Deng, Xingtao Yang, Haoyu Lu, Dacheng  
 789 Yin, Fengyun Rao, Minfeng Zhu, et al. R1-onevision: Advancing generalized multimodal reason-  
 790 ing through cross-modal formalization. *arXiv preprint arXiv:2503.10615*, 2025.

791

792 Yixin Ye, Zhen Huang, Yang Xiao, Ethan Chern, Shijie Xia, and Pengfei Liu. Limo: Less is more  
 793 for reasoning, 2025. URL <https://arxiv.org/abs/2502.03387>.

794

795 Qiyi Yu, Zheng Zhang, Ruofei Zhu, Yufeng Yuan, Xiaochen Zuo, Yu Yue, Tiantian Fan, Gaohong  
 796 Liu, Lingjun Liu, Xin Liu, et al. Dapo: An open-source llm reinforcement learning system at  
 797 scale. *arXiv preprint arXiv:2503.14476*, 2025.

798

799 Xiang Yue, Yuansheng Ni, Kai Zhang, Tianyu Zheng, Ruoqi Liu, Ge Zhang, Samuel Stevens,  
 800 Dongfu Jiang, Weiming Ren, Yuxuan Sun, Cong Wei, Botao Yu, Ruibin Yuan, Renliang Sun,  
 801 Ming Yin, Boyuan Zheng, Zhenzhu Yang, Yibo Liu, Wenhao Huang, Huan Sun, Yu Su, and  
 802 Wenhua Chen. Mmmu: A massive multi-discipline multimodal understanding and reasoning  
 803 benchmark for expert agi. In *Proceedings of CVPR*, 2024a.

804

805 Xiang Yue, Tianyu Zheng, Yuansheng Ni, Yubo Wang, Kai Zhang, Shengbang Tong, Yuxuan Sun,  
 806 Botao Yu, Ge Zhang, Huan Sun, et al. Mmmu-pro: A more robust multi-discipline multimodal  
 807 understanding benchmark. *arXiv preprint arXiv:2409.02813*, 2024b.

808

809 Weihao Zeng, Yuzhen Huang, Wei Liu, Keqing He, Qian Liu, Zejun Ma, and Junxian He. 7b model  
 810 and 8k examples: Emerging reasoning with reinforcement learning is both effective and efficient.

811

812 Ge Zhang, Xinrun Du, Bei Chen, Yiming Liang, Tongxu Luo, Tianyu Zheng, Kang Zhu, Yuyang  
 813 Cheng, Chunpu Xu, Shuyue Guo, Haoran Zhang, Xingwei Qu, Junjie Wang, Ruibin Yuan, Yizhi  
 814 Li, Zekun Wang, Yudong Liu, Yu-Hsuan Tsai, Fengji Zhang, Chenghua Lin, Wenhao Huang,  
 815 Wenhua Chen, and Jie Fu. CMMU: A chinese massive multi-discipline multimodal under-  
 816 standing benchmark. *CoRR*, abs/2401.11944, 2024a. doi: 10.48550/ARXIV.2401.11944. URL  
 817 <https://doi.org/10.48550/arXiv.2401.11944>.

810 Kaiyan Zhang, Yuxin Zuo, Bingxiang He, Youbang Sun, Runze Liu, Che Jiang, Yuchen Fan, Kai  
 811 Tian, Guoli Jia, Pengfei Li, et al. A survey of reinforcement learning for large reasoning models.  
 812 *arXiv preprint arXiv:2509.08827*, 2025a.

813

814 Renrui Zhang, Dongzhi Jiang, Yichi Zhang, Haokun Lin, Ziyu Guo, Pengshuo Qiu, Aojun Zhou,  
 815 Pan Lu, Kai-Wei Chang, Yu Qiao, et al. Mathverse: Does your multi-modal ILM truly see the  
 816 diagrams in visual math problems? In *European Conference on Computer Vision*, pp. 169–186.  
 817 Springer, 2024b.

818 Renrui Zhang, Xinyu Wei, Dongzhi Jiang, Ziyu Guo, Yichi Zhang, Chengzhuo Tong, Jiaming Liu,  
 819 Aojun Zhou, Shanghang Zhang, Peng Gao, and Hongsheng Li. MAVIS: mathematical visual  
 820 instruction tuning with an automatic data engine. In *The Thirteenth International Conference  
 821 on Learning Representations, ICLR 2025, Singapore, April 24-28, 2025*. OpenReview.net, 2025b.  
 822 URL <https://openreview.net/forum?id=MnJzJ2gvuf>.

823 Ruohong Zhang, Bowen Zhang, Yanghao Li, Haotian Zhang, Zhiqing Sun, Zhe Gan, Yinfei Yang,  
 824 Ruoming Pang, and Yiming Yang. Improve vision language model chain-of-thought reasoning,  
 825 2024c. URL <https://arxiv.org/abs/2410.16198>.

826

827 Yaowei Zheng, Richong Zhang, Junhao Zhang, Yanhan Ye, Zheyuan Luo, Zhangchi Feng, and  
 828 Yongqiang Ma. Llamafactory: Unified efficient fine-tuning of 100+ language models. In *Pro-  
 829 ceedings of the 62nd Annual Meeting of the Association for Computational Linguistics (Volume 3:  
 830 System Demonstrations)*, Bangkok, Thailand, 2024. Association for Computational Linguistics.  
 831 URL <http://arxiv.org/abs/2403.13372>.

832 Yaowei Zheng, Junting Lu, Shenzhi Wang, Zhangchi Feng, Dongdong Kuang, and Yuwen Xiong.  
 833 Easyr1: An efficient, scalable, multi-modality rl training framework. <https://github.com/hiyouga/EasyR1>, 2025.

834

835 Chengke Zou, Xingang Guo, Rui Yang, Junyu Zhang, Bin Hu, and Huan Zhang. Dynamath: A  
 836 dynamic visual benchmark for evaluating mathematical reasoning robustness of vision language  
 837 models, 2025. URL <https://arxiv.org/abs/2411.00836>.

838

839

840

841

842

843

844

845

846

847

848

849

850

851

852

853

854

855

856

857

858

859

860

861

862

863

**Table 5:** Key Hyperparameters for Training Stages.

Component	Hyperparameter	Component	Hyperparameter
<b>Cold Start</b>	Learning Rate = $2.0 \times 10^{-5}$	<b>Actor</b>	Global Batch Size = 128
	Gradient Accumulation = 8		Micro Batch Rollout = 4
	Number of Epochs = 5		Max Grad Norm = 1.0
	LR Scheduler = Cosine		Learning Rate (lr) = $1 \times 10^{-6}$
	Warmup Ratio = 0.05		Weight Decay = $1 \times 10^{-2}$
	Max Sequence Length = 32768		Entropy Coef Init ( $\beta_0$ ) = 0.02
	Precision = BF16		Entropy Coef Min ( $\beta_{\min}$ ) = 0.0
	DeepSpeed = Zero2		Entropy Decay Rate ( $\lambda$ ) = 0.985 (exp)
			Entropy Warmup Steps ( $\tau_w$ ) = 140
			Total Updates = 200000
<b>GRPO</b>	Adv Estimator = grpo	<b>Model Settings</b>	Max Prompt Length = 8192
	KL Penalty Type = low var kl		Max Response Length = 8192
	KL Coef = $2 \times 10^{-3}$		Rollout Batch Size = 512
	$\tau = 0.3$		Generation Temperature = 1.0
			Generation Top P = 0.95

## APPENDIX

### APPENDIX CONTENTS

<b>A LLM Usage Statement</b>	<b>17</b>
<b>B Training settings</b>	<b>17</b>
<b>C Algorithm in Prioritized Advantage Distillation (PAD)</b>	<b>17</b>
<b>D Reasoning Example</b>	<b>18</b>

### A LLM USAGE STATEMENT

In this paper, we employed a Large Language Model (LLM) in an assistive capacity for this manuscript. Its use was strictly limited for grammatical accuracy and refining sentence structure to improve clarity and readability. All intellectual contributions, including the formulation of ideas, data analysis, and the composition of the manuscript, are entirely the work of the authors.

### B TRAINING SETTINGS

The training process can be divided into three distinct phases: cold start, multimodal reinforcement learning, and text-only reinforcement learning. Key hyperparameters for each training phase are detailed in Table 5.

### C ALGORITHM IN PRIORITIZED ADVANTAGE DISTILLATION (PAD)

The PAD mechanism, introduced conceptually in the main text, is detailed in Algorithm 1 to clarify its step-by-step operation in refining training batches for more effective learning.

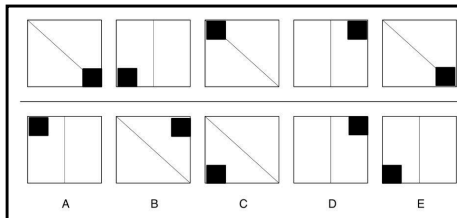
Initially, PAD filters the original batch  $\mathcal{B}$  to create an “effective set”  $\mathcal{E}$  of sample indices and a corresponding map  $\hat{A}_{\mathcal{E}}$  for their advantages (Lines 2-10 in Algorithm 1). For each sequence  $i$  in  $\mathcal{B}$ , its absolute advantage  $|\hat{A}_i|$  is computed. If this value falls within a specified informative range  $[T_{low}, T_{high}]$ , where  $T_{low} > 0$  is crucial for excluding stagnant (near-zero advantage) samples, the index  $i$  is added to  $\mathcal{E}$ , and its absolute advantage  $\hat{A}_{i,abs}$  is stored in  $\hat{A}_{\mathcal{E}}$ .

918 **Table 6:** Performance comparison on general textual and multimodal benchmarks. Best results per group (3B  
 919 or 7B) are **bold**, and second-best per group (3B or 7B) are underlined.

Model	MMMU	MMMU-PRO	CMMMU	MMStar	MMLU-Pro	Avg.
<i>3B Models</i>						
Qwen2.5-VL-3B-Instruct	49.78	32.64	<u>45.93</u>	51.61	41.24	44.64
FAST-3B	<u>52.00</u>	<u>34.61</u>	44.58	<b>55.15</b>	<u>44.06</u>	46.48
VLAA-Thinker-3B	49.67	33.34	44.92	53.35	42.35	44.33
<b>Revisual-R1-3B</b>	<b>64.78</b>	<b>44.47</b>	<b>51.19</b>	<u>53.76</u>	<b>51.82</b>	<b>53.60</b>
<i>7B Models</i>						
Qwen2.5-VL-7B-Instruct	52.00	42.52	51.69	61.71	51.80	51.94
ThinkLite-7B-VL	53.00	41.01	50.51	<b>64.73</b>	52.74	52.34
VL-Rethinker-7B	<u>59.78</u>	<u>45.59</u>	<u>52.54</u>	63.92	53.31	<u>55.03</u>
MM-Eureka-Qwen-7B	56.22	43.50	52.20	<u>64.16</u>	<u>54.03</u>	54.17
<b>Revisual-R1-7B</b>	<b>67.00</b>	<b>54.35</b>	<b>56.95</b>	63.86	<b>62.38</b>	<b>60.91</b>

934 If this effective set  $\mathcal{E}$  is non-empty, prioritized sub-sampling is performed (Lines 12-29). This multi-  
 935 step process involves: (a) Calculating sampling probabilities  $P_j$  for each sequence index  $j \in \mathcal{E}$  via a  
 936 temperature-controlled Softmax distribution over their stored absolute advantages  $\hat{A}_{\mathcal{E}}[j]$  (Lines 14-  
 937 21). A uniform probability distribution across  $\mathcal{E}$  serves as a fallback mechanism should the Softmax  
 938 normalization term  $Z$  be zero. (b) Determining the sub-sample size  $k'$  as  $\min(\lceil \rho N \rceil, |\mathcal{E}|)$ , where  $\rho$   
 939 is the sub-sampling ratio and  $N$  is the original batch size (Line 23). (c) Sampling  $k'$  indices from  
 940  $\mathcal{E}$  according to the calculated probabilities  $P_{\text{dist}}$  (Line 25). (d) Constructing the final distilled mini-  
 941 batch  $\mathcal{B}_{\text{distilled}}$  by retrieving the original sequences corresponding to these  $k'$  sampled indices (Lines  
 942 27-29). If  $\mathcal{E}$  is void, an empty batch is returned. This entire procedure ensures that training batches  
 943 are enriched by systematically filtering out uninformative data and prioritizing samples anticipated  
 944 to yield more substantial learning signals.

## D REASONING EXAMPLE

972  
973  
974  
975  
976  
977  
978  
979

Question:

Which of the boxes comes next  
in the sequence?

Select answers from A-E

980

Ours Revisual-R1 7B Model:

&lt;think&gt;

Okay, let's try to figure out the sequence here. So there are five options labeled A to E, each with some black squares in different positions. The problem is asking which one comes next in the sequence.

First, I need to look at the given figures and see if there's a pattern. Let me list them out again to make sure I have them right, Top row:  
 1. A: A square divided by a diagonal, with a black square in the bottom right corner.  
 2. B: Two vertical stripes, each with a black square on the right side.  
 3. C: A square with a diagonal from top left to bottom right, and a black square in the top left quadrant.  
 4. D: Two vertical stripes, with a black square in the right stripe's upper part.  
 5. E: A square split into two vertical parts, with a black square in the left part.

[Reflection] Wait, maybe I should number them as per their order in the problem. The first row is options 1 to 5, then the second row is A to E. Wait, the problem shows the first row as the original five, then the next row labeled A to E.

[Revisit Image] Wait, looking back: The user presented the problem with two rows. The first row has five images (probably labeled 1 to 5), but the user then labels the second row as A to E. Wait, the actual question's options are A to E, each in the second row.

The sequence seems to involve the placement of the black squares relative to the diagonals or divisions of the square. Let me analyze each option:

Original top row (before the line).....

Then the next row is labeled A to E: A: Square split vertically, left third has a black square.....

[Self-Critic] Wait, perhaps the original problem's figures are arranged as follows:

First row (top): .....

Second row (labeled A to E): A: Vertical division, left part has a black square.....

[Logic] Now, trying to see the pattern. Let's look at the original figures (before the line) and then the options A-E. The task is to determine which comes next. Looking at the first row's figures (original positions):.....

[Self-Critic] Wait, maybe the pattern alternates between diagonal and vertical splits. Let's check:

Original sequence (top row): 1. Diagonal, lower right.....

Then the next row (A-E): A: Vertical split (three parts?), left part black.....

If the pattern is alternating between diagonal and vertical splits, then after figure 5 (diagonal), the next would be a vertical split.

[Hypothesis] Looking at the original vertical splits: figures 2, 4, and then maybe A, D, E.

Let's see: Original vertical splits (two parts) are figures 2 (lower right), 4 (upper right). Then after figure 5 (diagonal), next could be another vertical split. Among options A-E, which are vertical splits: A: vertical split into three columns? Or two columns? The image for A is a square split vertically into left and right, with a black square in the left part. D is vertical split into two, with black in the right upper. E is vertical split into two, black in left lower.

So after figure 5 (diagonal), the next might be a vertical split. The last vertical split in the original sequence (figure 4) has the black square in the upper right. Then the next vertical split could be in the lower left (E) or upper left (A?), but need to check the order.

[Hypothesis & Analysis] Alternatively, looking at the positions: Original vertical splits: Figure 2: right lower. Figure 4: right upper.

So if the pattern for vertical splits is alternating between lower and upper in the right section, then next could be lower right again? But figure 2 is right lower, figure 4 is right upper. So maybe the next vertical split would be right lower again. Then option E is left lower. Hmm, not sure.

Alternatively, maybe the sequence is moving in a certain direction. Let's think of the figures as arranged in rows. The first row has five figures, and the second row has A-E. The correct answer is among A-E, which are the second row.

[Hypothesis] Alternatively, the sequence might be based on rotation or the position of the black square. For example, starting with diagonal, then vertical splits. Let's see:.... Wait, the options A-E are all vertical splits except B and C, which have diagonals. Wait, original figures 1-5 have a mix: 1,3,5 have diagonals; 2,4 have vertical splits. The options A-E: A is vertical split left; B is diagonal with black in upper right; C is diagonal upper left; D is vertical split right upper; E is vertical split left lower.

So after figure 5 (diagonal lower right), the next figure is likely a vertical split. Now, in the original vertical splits (figures 2 and 4), figure 2 is right lower, figure 4 is right upper. So maybe the next vertical split alternates. If figure 4 was right upper, then next could be right lower again (figure 2's position).

[Reflection] But option E is left lower. Hmm. Alternatively, the vertical splits in the original sequence go from right lower to right upper. If the next vertical split is right lower again, but that's figure 2. But E is left lower.

[Hypothesis] Alternatively, maybe the direction is moving left.

Wait, maybe the pattern is that after two diagonal figures (1,3,5), the vertical splits alternate between right and left. Let's see: Original vertical splits: figure 2 (right lower), figure 4 (right upper). Then the next vertical split might be left lower (E) or left upper (A). But figure A is left black square, which is a vertical split left. If the pattern is moving from right to left, then after figure 4 (right upper), next would be left lower (E).

[Self-Critic] But I need to check. Alternatively, looking at the positions of the black squares in the vertical splits: Figure 2: right third, lower part. Figure 4: right third, upper part.

So the vertical split's black square moves from lower to upper in the same right third. Then, if the next vertical split is in the left third, maybe lower part (E). So after moving right upper, next is left lower. That would make the pattern: right lower, right upper, left lower. So E. Alternatively, the answer is E.

[Self-Critic] Let's check the options: Original sequence: diagonal, vertical split (right lower), diagonal, vertical split (right upper), diagonal. Then next is vertical split (left lower, E). That seems plausible. Another way: looking at the positions of the black squares in the vertical splits. The vertical splits in figures 2 and 4 have the black square in the right third. Figure 2's black square is at the lower part of the right third, figure 4's is at the upper part.

So if we follow that pattern, the next vertical split would be in the left third, perhaps at the lower part (E). So the answer is E.

</think>

<summary>

The sequence involves alternating between diagonal and vertical split figures. After the diagonal figure (5), the next is a vertical split. The vertical splits in the original sequence (figures 2 and 4) have black squares in the right third, moving from lower to upper. The next vertical split follows this pattern but in the left third, at the lower part.

Answer: boxed{E}



</summary>

**Figure 5:** Our Revisual-R1 model reasoning case, showcasing its exceptional reasoning ability. The model generates long responses, continuously hypothesizing, reflecting, verifying, and correcting to arrive at the final answer, while also providing a summary answer.

1026

1027

1028

1029

1030

1031

1032

1033

1034

1035

1036

1037

**Algorithm 1** Prioritized Advantage Distillation (PAD)

1038 **Require:** Original batch  $\mathcal{B} = \{seq_1, \dots, seq_N\}$  with  $N = |\mathcal{B}|$ ; advantage estimates  $A_{\text{est}} = \{\tilde{A}_1, \dots, \tilde{A}_N\}$ ;  
 1039 thresholds  $T_{\text{low}}, T_{\text{high}}$ ; temperature  $\tau$ ; subsampling ratio  $\rho$

1040 **Ensure:** Distilled minibatch  $\mathcal{B}_{\text{distilled}}$

▷ **Steps 1 & 2: Per-Sequence Advantage Calculation and Effective Sample Filtering**

1041 1:  $\mathcal{E} \leftarrow \emptyset$  ▷ Set of indices for effective samples  
 1042 2:  $\hat{A}_{\mathcal{E}} \leftarrow \{\}$  ▷ Map: original index  $i \in \mathcal{E}$   $\rightarrow$  its absolute advantage  $\hat{A}_i$   
 1043 3: **for**  $i \leftarrow 1$  **to**  $N$  **do** ▷ Absolute advantage of current sequence  $i$   
 1044 4:    $\hat{A}_{i,abs} \leftarrow |\tilde{A}_i|$   
 1045 5:   **if**  $T_{\text{low}} \leq \hat{A}_{i,abs} \leq T_{\text{high}}$  **then** ▷ Add index to effective set  
 1046 6:      $\mathcal{E} \leftarrow \mathcal{E} \cup \{i\}$   
 1047 7:      $\hat{A}_{\mathcal{E}}[i] \leftarrow \hat{A}_{i,abs}$  ▷ Store absolute advantage for effective sample  $i$   
 1048 8:   **end if**  
 1049 9: **end for**  
 1050 10:  $\mathcal{B}_{\text{distilled}} \leftarrow \emptyset$   
 1051 11: **if**  $|\mathcal{E}| > 0$  **then** ▷ **Step 3: Prioritized Sub-sampling from the Effective Set**  
 1052   12:  $Z \leftarrow \sum_{j \in \mathcal{E}} \exp(\hat{A}_{\mathcal{E}}[j]/\tau)$  ▷ a. Calculate sampling probabilities  $P_j$  for each  $j \in \mathcal{E}$   
 1053   13:  $P_{\text{dist}} \leftarrow \{\}$  ▷ Normalization term (Softmax denominator over  $\mathcal{E}$ )  
 1054   14: **for all**  $j \in \mathcal{E}$  **do** ▷ Map: original index  $j \in \mathcal{E}$   $\rightarrow$  its sampling probability  $P_j$   
 1055   15:   **if**  $Z > 0$  **then** ▷ b. Determine actual sub-sample size  $k'$   
 1056   16:      $P_{\text{dist}}[j] \leftarrow \exp(\hat{A}_{\mathcal{E}}[j]/\tau)/Z$   
 1057   17:   **else** ▷ Uniform fallback if  $Z = 0$   
 1058   18:      $P_{\text{dist}}[j] \leftarrow 1/|\mathcal{E}|$   
 1059   19:   **end if**  
 1060   20: **end for** ▷ c. Sample  $k'$  indices from  $\mathcal{E}$  according to probabilities  $P_{\text{dist}}$   
 1061   21:  $k' \leftarrow \min(\lceil \rho N \rceil, |\mathcal{E}|)$  ▷ d. Form the distilled mini-batch  
 1062   22:  $S_{\text{sampled\_indices}} \leftarrow \text{SAMPLE}(\mathcal{E}, P_{\text{dist}}, k')$  ▷  $S_{\text{sampled\_indices}}$  is a list of  $k'$  indices from  $\mathcal{E}$   
 1063   23: **for all**  $idx \in S_{\text{sampled\_indices}}$  **do**  
 1064   24:    $\mathcal{B}_{\text{distilled}} \leftarrow \mathcal{B}_{\text{distilled}} \cup \{seq_{idx}\}$   
 1065   25: **end for**  
 1066   26: **end if**  
 1067   27: **return**  $\mathcal{B}_{\text{distilled}}$

1070

1071

1072

1073

1074

1075

1076

1077

1078

1079